ChemComm

RSC Publishing

COMMUNICATION

View Article Online
View Journal | View Issue

Cite this: *Chem. Commun.*, 2013, **49**, 7334

Received 17th June 2013,
Accepted 22nd June 2013

DOI: 10.1039/c3cc44517h

www.rsc.org/chemcomm

Design of an anti-aggregated SERS sensing platform for metal ion detection based on bovine serum albumin-mediated metal nanoparticles†

Wei Ji,[ab] Lei Chen,[a] Xiangxin Xue,[a] Zhinan Guo,[a] Zhi Yu,[a] Bing Zhao*[a] and Yukihiro Ozaki*[b]

Based on bovine serum albumin (BSA)-modified Au NPs, a simple and cost-effective approach was proposed to fabricate an anti-aggregated Au NP sensing platform for the detection of metal ions. It exhibits excellent stability even under highly ionic conditions due to its electrostatic stabilization, as well as the steric stabilization.

As the environmental issue being concerned increasingly, many countries are now making great effort to curb pollution and monitor contaminants in water, air, and foods. Surface-enhanced Raman scattering (SERS) spectroscopy is one of the most ultrasensitive molecular spectroscopy techniques, and thus it can be used to detect contaminants at femtomolar concentrations over practical monitoring scales.[1–3] Recently, numerous designs of SERS sensors based on metal nanoparticles (NPs) or metallic nanostructures have been proposed for the detection of small inorganic molecules and ions.[4–7] Such studies are typically carried out by direct identification of the vibrational fingerprint of the inorganic probe molecules or by monitoring changes in a pre-adsorbed molecule through interaction with the inorganic probe species. Despite the promising results achieved, development of such SERS sensors for practical test requirements is still an important challenge. As we all know, the chemical complexity of a practical sample (*e.g.*, sewage, seawater, and whole blood) inevitably leads to different aggregations of SERS-sensors from sample-to-sample. The extent of aggregation of the metal nanoparticles could give rise to dramatic enhancement or even changes in the adsorbed molecule's SERS signal.[8–10] Therefore, the uncontrollable aggregation of SERS-active substrates disturbs severely the quantitative analysis of environmental, industrial and biological samples.

Herein, we have provided a simple and effective protocol for fabricating anti-aggregated SERS sensors to detect inorganic ions using bovine serum albumin (BSA)-modified Au NPs. BSA is used because of its stability to resist NP aggregation in assays, its lack of SERS signal that avoids signal interference with the probe molecule, and its low cost. Scheme 1 illustrates the preparation protocol of the proposed sensor and its application in ion detection. BSA can bind to gold NPs by the strong interactions such as hydrophobic, electrostatic, and covalent interactions.[11] The two typical approaches for test ions are discussed in this work as examples. Thus, *p*-aminobenzenethiol (PATP) and rhodamine 6G (R6G) were used as SERS reporters for determination of Ag^+ and Hg^{2+} ions, respectively. PATP is a one of the most popular molecules in the study of the chemical enhancement mechanism because of its high-quality signal and unusual performance.[12–14] It can adsorb on the surface of Au NPs *via* the formation of Au–S bonds and interact with Ag^+ ions *via* primary amines. The interaction results in the selective enhancement of the b_2-type band intensities of PATP. R6G adsorbs on the surface of Au NPs *via* the electrostatic interaction.[15] This adsorption causes R6G to be displaced more easily from the surface of Au NPs by Hg^{2+} ions due to the strong affinity between Au and Hg^{2+},[16,17] subsequently leading to the decrease in SERS intensities of R6G. The effects of introduced BSA on the stability, sensitivity, and selectivity of our proposed probe-Au@BSA sensing platform have been evaluated. We further validated the practicality of this proposed SERS sensing platform through the detection of Ag^+ and Hg^{2+} in real water samples.

Fig. S1 (ESI†) shows the transmission electron microscopy (TEM) images of the Au NPs, and the proposed BSA-modified probe-Au NPs.

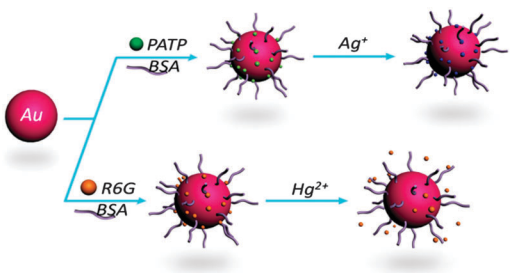

Scheme 1 Schematic diagram representing the formation of the anti-aggregated SERS sensor and its response mechanism for Ag^+ and Hg^{2+}, respectively.

[a] *State Key Laboratory of Supramolecular Structure and Materials, Jilin University, Changchun, 130012, P. R. China. E-mail: zhaob@mail.jlu.edu.cn; Fax: +86 431 8519 3421; Tel: +86 431 8516 8473*

[b] *Department of Chemistry, School of Science and Technology, Kwansei Gakuin University, Sanda, Hyogo, 669-1337, Japan. E-mail: ozaki@kwansei.ac.jp; Fax: +81 79 565 9077; Tel: +81 79 565 8349*

† Electronic supplementary information (ESI) available: Experimental procedures and additional figures. See DOI: 10.1039/c3cc44517h

Because BSA is composed of carbon, hydrogen, oxygen, nitrogen and other light elements, the electron beam almost completely travels through the specimen, which gives rise to low contrast in the TEM images, making them difficult to identify. It is worth noting that the Au NPs are attached to each other in an original case (Fig. S1, ESI†). However, after having been modified with BSA, it can be clearly seen that the Au NPs exist nearly in a monodisperse state. The relatively nearby distance distributions are ~2.3 and ~1.5 nm between two NPs in PATP-Au@BSA and R6G-Au@BSA, respectively. According to the dynamic light scattering measurement, their hydrodynamic diameters increased after modification with BSA, further indicating that protein corona was formed around the Au NPs (Fig. S2, ESI†). Moreover, a slight red-shift in the surface plasmon resonance absorbance of Au NPs also implies that BSA is adsorbed on the surface of Au NPs (Fig. 1).

The citrate-reduced Au NPs readily aggregate under highly ionic conditions, especially in a metal halide salt. The UV-vis-NIR absorption spectra in the absence and presence of 1 M NaCl shown in Fig. 1 enable us to explore the stability of our proposed probe-Au@BSA sensing platform. The surface plasmon absorption band of the Au NPs is located at 519 nm. The addition of NaCl results in a loss of intensity of the original absorption peak as well as the occurrence of a new broad band at around 730 nm, arising from the plasmon resonance of aggregates (Fig. S4, ESI†). Similarly, both PATP-Au and R6G-Au exhibit aggregation to variable extents as well. However, there is no obvious change in the absorption profile of BSA protected Au NPs. The corresponding TEM images also suggest that the introduction of BSA was an effective measure to inhibit the Au NP aggregation (Fig. S5, ESI†). In general, the electrostatically stable Au NPs will fail to stabilize in response to introduction of the electrolyte. In contrast to electrostatic stabilization alone, BSA contains abundant side chains and domains, which result in steric stabilization giving more stable performance.[11,18,19]

SERS intensities of analytes are susceptible to metal NP aggregates because the strong enhancement occurs in the narrow gap of two closely approaching NPs (forming the so-called "hot spot") owing to electromagnetic coupling between the neighboring metal NPs. On the other hand, excessive aggregation may lead to decay of SERS intensities as well. To explore its anti-aggregation effect in SERS detection, the SERS spectra of the proposed sensing platform in the absence and presence of different concentrations of NaCl are shown in Fig. 2.

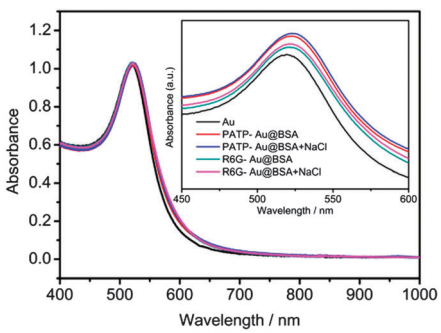

Fig. 1 UV-vis-NIR absorption spectra of Au NPs, PATP-Au@BSA, and R6G-Au@BSA in the absence and presence of 1 M NaCl. The inset shows the enlarged spectra ranging from 450 to 600 nm, the correlating absorbance was adjusted for detailed analysis.

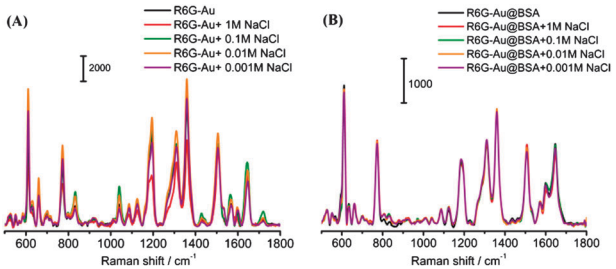

Fig. 2 The SERS spectra of (A) R6G-Au and (B) R6G-Au@BSA in the absence and presence of different amounts of NaCl.

The SERS intensities of R6G-Au exhibit dramatic fluctuations due to the aggregation to variable extents. Nevertheless, SERS intensities of R6G-Au@BSA are almost the same as that without addition of NaCl. For detailed analysis, the variation in the intensity of the typical band at 610 cm^{-1} is shown in Fig. S6 (ESI†). It is clearly found that the SERS intensity of R6G in the R6G-Au@BSA sensing platform exhibits excellent stability in spite of its intensity decrease after the introduction of BSA into this system. This indicates that the BSA modified Au NPs are highly stable even under highly ionic conditions.

Considering that excess BSA would bind with metal ions to some extent, centrifuge purification was carried out to obtain higher sensitivity. After centrifugation, the R6G-Au@BSA sensing platform was used to detect the Hg^{2+} ions. As shown in Fig. 3, SERS intensities are decreased with the addition of Hg^{2+} ions because R6G is displaced from the surface of Au NPs by Hg^{2+} ions due to the special affinity between Au and Hg^{2+}.[16,17] Moreover, the as prepared R6G-Au@BSA sensing platform exhibited greater selectivity and lower interference toward Hg^{2+} ions (Fig. S7, ESI†). It is found that the concentration to quantify Hg^{2+} ions can be down to 0.1 ppb (Fig. S8, ESI†), which is consistent with a previous report.[15] Our results indicate that BSA absorbed on the surface of Au NPs rarely affects the metal ion detection. It may arise from two main causes: firstly, only small amounts of BSA are adsorbed on the surface of Au NPs. Secondly, the cysteine residues are buried in the intact structure of the protein, and thus it cannot combine with a lot of metal ions. Meanwhile, the Ag^{+} ion response experiment shown in Fig. 4 is further evidence suggesting that introduced BSA has a limited impact on metal ion detection.

The SERS spectra of the PATP-Au@BSA sensing platform as a function of Ag^{+} ions are shown in Fig. 4, where the concentration of Ag^{+} ions ranges from 0 to 1.0 ppm. In the absence of Ag^{+}, the predominant bands are located at 1004, 1077, 1173, 1486, 1585, and 1631 cm^{-1}, which have been assigned to the a_1 modes of the PATP

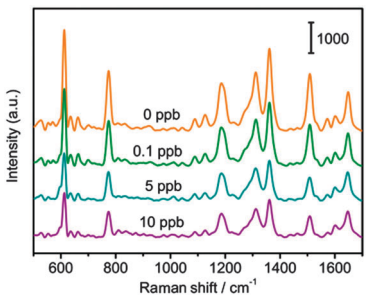

Fig. 3 Concentration-dependent SERS spectra of the R6G-Au@BSA sensing platform in the presence of Hg^{2+} ions ranging from 0 to 10 ppb.

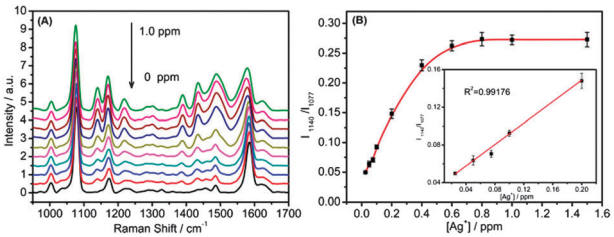

Fig. 4 (A) SERS spectra of the as-prepared PATP-Au@BSA sensing platform in the absence and presence of Ag^+ ions (the concentration from the bottom to the top is 0, 0.025, 0.05, 0.075, 0.1, 0.2, 0.4, 0.6, 0.8, and 1.0 ppm, respectively). (B) Relative band intensities (I_{1140}/I_{1077}) *versus* the concentration of Ag^+ ions.

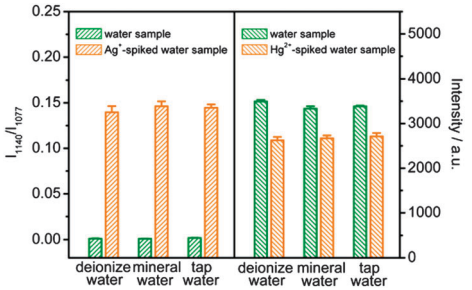

Fig. 5 SERS response of PATP-Au@BSA (left) and R6G-Au@BSA (right) to different water samples and water samples spiked with 0.2 ppm Ag^+ or 0.5 ppb Hg^{2+}, respectively.

molecule.[12] However, a remarkable change appeared in the bands at 1104, 1217, 1389, and 1435 cm^{-1} which are selectively enhanced upon addition of Ag^+ ions. These bands have been assigned to the b_2 modes of the PATP molecule. The changes in the relative intensities of the two type bands probably arise from the Herzberg–Teller contribution *via* charger-transfer.[12,13,20] We selected two representative bands, a typical a_1-type band at $\sim$1077 cm^{-1}, and a b_2-type band at $\sim$1140 cm^{-1}, for analysis of the concentration-dependent variation. As shown in Fig. 4B, the intensity ratio increases with increasing the amount of Ag^+ and reaches a maximum value at the concentration of 0.6 ppm. A linear correlation existed between the value of I_{1140}/I_{1078} and the concentration of 0.2–0.025 ppm. Moreover, the response of PATP-Au@BSA to the presence of various environment-related metal ions was investigated (Fig. S9, ESI†). Our results indicate that the as-prepared PATP-Au@BSA sensing platform displays a remarkably high selectivity for Ag^+ ions.

To evaluate the capability of this proposed SERS sensing platform for the detection of metal ions in real water samples, we examined the SERS response of Hg^{2+} and Ag^+ ions in deionized water, tap water, and mineral water, respectively. Prior to the preparation of spiked water, all samples were filtered through a 0.22 μm membrane to remove any particulate suspension. Because natural water usually contains small amounts of Hg^{2+} or Ag^+ ions, they are not detected in our samples (Fig. 5). However, a significant response was observed in the SERS spectra when the water samples were spiked with 0.2 ppm Ag^+ or 0.5 ppb Hg^{2+}. As shown in Fig. 5, there were almost the same changes for different spiked water samples. In these measurements, the recovery of Ag^+ ions for the three samples was 94.83–100.88% and of Hg^{2+} ions was 94.37–116.02% (Table S1, ESI†), which further reveals that our proposed BSA modified sensing platform has a significant advantage in practical sample applications.

In summary, a simple and cost-effective approach for fabricating an anti-aggregated Au NP sensing platform has been proposed for quantitatively monitoring metal ions by SERS. BSA was used as a stabilizer because it is easy to obtain and stabilized by the interaction of protein side chains or domains in addition to its electrostatic stabilization, thereby the PATP-Au@BSA and R6G-Au@BSA sensing platforms were highly stable even under highly ionic conditions. The results described in this paper show that the proposed sensing platform is effective in monitoring the Ag^+ and Hg^{2+} ions in real water samples. Moreover, other metal ions can also be detected by substituting PATP or R6G with other native or artificial probes that selectively respond to the analyte. The promising technique with its advantages of simplicity, cost-effectiveness, and universality has great potential for reliable detection of metal ions in food, water, and biological samples.

This research was supported by the National Natural Science Foundation (20921003, 20973074) of P. R. China; Specialized Research Fund for the Doctoral Program of Higher Education (20110061110017); the 111 project (B06009); and the Development Program of the Science and Technology of Jilin Province (20110338).

Notes and references

1 R. A. Halvorson and P. J. Vikesland, *Environ. Sci. Technol.*, 2010, **44**, 7749–7755.
2 J. F. Li, Y. F. Huang, Y. Ding, Z. L. Yang, S. B. Li, X. S. Zhou, F. R. Fan, W. Zhang, Z. Y. Zhou, D. Y. Wu, B. Ren, Z. L. Wang and Z. Q. Tian, *Nature*, 2010, **464**, 392–395.
3 Y. Xie, X. Wang, X. Han, X. Xue, W. Ji, Z. Qi, J. Liu, B. Zhao and Y. Ozaki, *Analyst*, 2010, **135**, 1389–1394.
4 S. J. Lee and M. Moskovits, *Nano Lett.*, 2010, **11**, 145–150.
5 Y. Wang and J. Irudayaraj, *Chem. Commun.*, 2011, **47**, 4394–4396.
6 J. Yin, T. Wu, J. Song, Q. Zhang, S. Liu, R. Xu and H. Duan, *Chem. Mater.*, 2011, **23**, 4756–4764.
7 R. A. Alvarez-Puebla and L. M. Liz-Marzán, *Angew. Chem., Int. Ed.*, 2012, **51**, 11214–11223.
8 S. E. J. Bell and N. M. S. Sirimuthu, *J. Phys. Chem. A*, 2005, **109**, 7405–7410.
9 X. X. Han, G. G. Huang, B. Zhao and Y. Ozaki, *Anal. Chem.*, 2009, **81**, 3329–3333.
10 K. Kim, Y. M. Lee, H. B. Lee, Y. Park, T. Y. Bae, Y. M. Jung, C. H. Choi and K. S. Shin, *J. Raman Spectrosc.*, 2010, **41**, 187–192.
11 S. H. Brewer, W. R. Glomm, M. C. Johnson, M. K. Knag and S. Franzen, *Langmuir*, 2005, **21**, 9303–9307.
12 M. Osawa, N. Matsuda, K. Yoshii and I. Uchida, *J. Phys. Chem.*, 1994, **98**, 12702–12707.
13 K. Kim, D. Shin, H. B. Lee and K. S. Shin, *Chem. Commun.*, 2011, **47**, 2020–2022.
14 W. Ji, N. Spegazzini, Y. Kitahama, Y. Chen, B. Zhao and Y. Ozaki, *J. Phys. Chem. Lett.*, 2012, **3**, 3204–3209.
15 G. Wang, C. Lim, L. Chen, H. Chon, J. Choo, J. Hong and A. J. deMello, *Anal. Bioanal. Chem.*, 2009, **394**, 1827–1832.
16 K. Leopold, M. Foulkes and P. J. Worsfold, *Anal. Chem.*, 2009, **81**, 3421–3428.
17 J. Xie, Y. Zheng and J. Y. Ying, *Chem. Commun.*, 2010, **46**, 961–963.
18 C. Guo and J. Irudayaraj, *Anal. Chem.*, 2011, **83**, 2883–2889.
19 Y. F. Lee, F. H. Nan, M. J. Chen, H. Y. Wu, C. W. Ho, Y. Y. Chen and C. C. Huang, *Anal. Methods*, 2012, **4**, 1709–1717.
20 J. R. Lombardi and R. L. Birke, *Acc. Chem. Res.*, 2009, **42**, 734–742.

